column. Using the average gas holdup, $\bar{\varepsilon}_g$, in the entire reactor as measured by DP, the resulting void fraction profiles, calculated for all three process conditions, are shown in Figure 2.8.

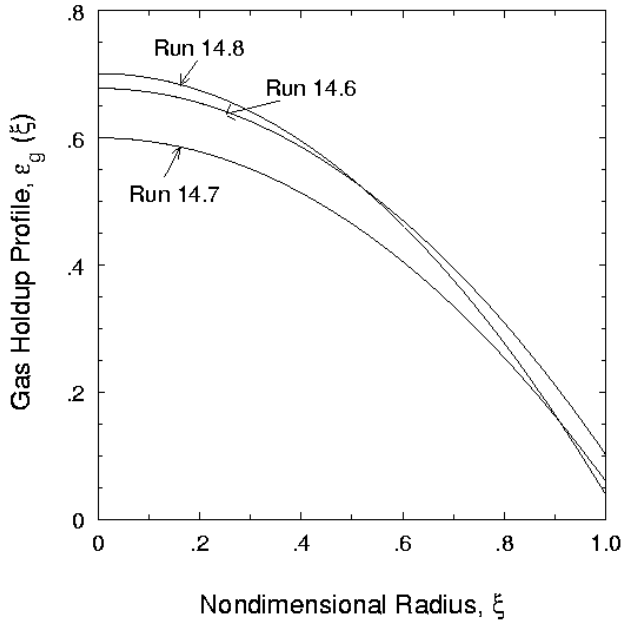

Figure 2.8 Radial Gas Holdup Profiles Calculated from Global Gas Holdup Measurements (DP and NDG) in the AFDU During Methanol Synthesis

2.4.3 Tracer Experiments

A schematic of the AFDU slurry bubble column reactor is shown in Figure 2.9. It has an internal diameter of 0.46 m and a height of 15.24 m, with the liquid - gas - solid dispersion level maintained at 13.25 m (L/D ratio of 28.8) during the runs discussed here. The vapor phase and liquid phase tracer experiments were conducted separately. Radioactive Ar-41, used to study the residence time distribution of the vapor phase, was injected as a pulse at the inlet of the reactor. Radioactive Manganese-56 (50 μm) particles mixed in oil were used for liquid (slurry) phase tracing. Four pulse injections were made at a given process rate: (1) lower nozzle N2 - 4.5 in. (11.4 cm) from wall, (2) nozzle N2 - at wall, (3) upper nozzle N1 - 4.5 in. (11.4 cm) from wall, and (4) nozzle N1 - at wall. The axial levels of these injection points are shown in Figure 2.9. The injections made at 4.5 in. (11.4 cm) from the wall are referred to as "center injections," as they are made into the core part of the column, where the liquid is known to move upward by convection in the time-averaged sense.

Radiation measurements from the vapor and liquid tracers were made using thirty 2" by 2" NaI scintillation detectors positioned outside the column at various axial levels, as shown in Figure 2.9. Sets of four detectors were placed at 90-degree angles at seven axial locations. In addition, detectors were placed at the inlet and outlet of the reactor. During the liquid tracer study, the

inlet detector was placed close to the liquid injection point to monitor the shape of the injected pulse.

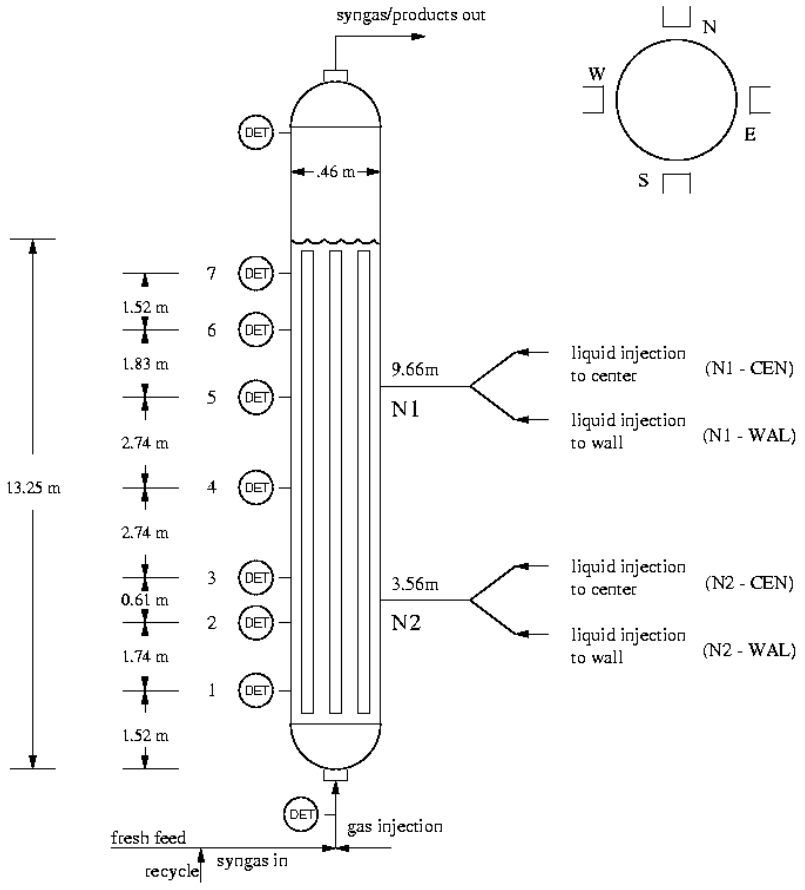

Figure 2.9 Schematic of Reactor for Tracer Experiments

The detectors were shielded on their sides, thereby allowing only the front circular surface of the detectors to be exposed to radiation. With this configuration, the spatial range from which a detector received most of its radiation was assessed. Details of these calculations are discussed in the fourth quarterly report for DOE (Degaleesan et al., 1996b). It has been shown that most of the intensity recorded at a detector, shielded on its sides, emanates from a slice of volume at the given axial level of the detector. For analyses purposes, only the tracer from the cross section of the reactor at the axial location of the detector is considered here.

2.4.4 Model Parameters

In order to use the current model to predict liquid tracer distribution in the column it is necessary to evaluate the model parameters. Experimental information exists only for the average gas holdup. From the holdup measurements using DP and NDG, there is an axial variation of the gas

holdup in the reactor due to reaction. This variation is not very significant as far as the slurry phase mixing is concerned, and as a first approximation, the average gas holdup in the reactor as obtained from DP measurements is considered. The corresponding radial gas holdup profiles calculated using results from DP and NDG are shown in Figure 2.8. Information on the other fluid dynamic variables, namely, the liquid velocity profile and turbulent eddy diffusivities, does not exist. Hence, the preliminary scaleup rules and characterization methodology were used to evaluate the mean liquid recirculating velocity and average turbulent eddy diffusivities. Since the current experimental conditions involve high pressure and a slurry system, this significantly alters the overall gas holdup in the reactor (Wilkinson et al. 1992), which for the present case results in gas holdups higher than that at atmospheric conditions for air-water systems. Knowing the average gas holdup in the reactor (Table 2.1), and using Equation 2.22, the equivalent gas velocity, U_{ge}, for the three operating conditions is calculated (shown in Table 2.3).

$$\bar{\varepsilon}_g = 0.07 U_g^{\,0.474 - 0.000626 D_c} \qquad \text{(in cgs units)} \tag{2.22}$$

For Run 14.6, U_{ge} = 47 cm/s, which is considerably higher than the original inlet gas velocity of 25 cm/s. The estimated U_{ge} is used in Equations 2.23 to 2.27, to evaluate the mean recirculation velocity and average axial and radial turbulent diffusivities under the existing conditions in the AFDU.

$$\bar{u}_{rec}(cm/s) = 2.2 D_c^{0.4} U_g^{0.4} \tag{2.23}$$

$$\overline{D}_{zz} = 2\int_0^1 D_{zz}(\xi)\xi d\xi \tag{2.24}$$

$$\overline{D}_{rr} = 2\int_0^1 D_{rr}(\xi)\xi d\xi \tag{2.25}$$

$$\overline{D}_{zz}(cm^2/s) = -\frac{2325}{D_c^{0.8}} + 106.6 D_c^{0.3} U_g^{0.3} \tag{2.26}$$

$$\overline{D}_{rr}(cm^2/s) = -\frac{350}{D_c^{0.8}} + 13.0 D_c^{0.3} U_g^{0.3} \tag{2.27}$$

The liquid recirculating velocity profile, $u_z(r)$, is then calculated by the procedure outlined in Figure 2.10, using as input the holdup profile estimated from DP and NDG measurements (Figure 2.8), and the knowledge of the mean recirculation velocity, $\bar{u}_{rec}$.

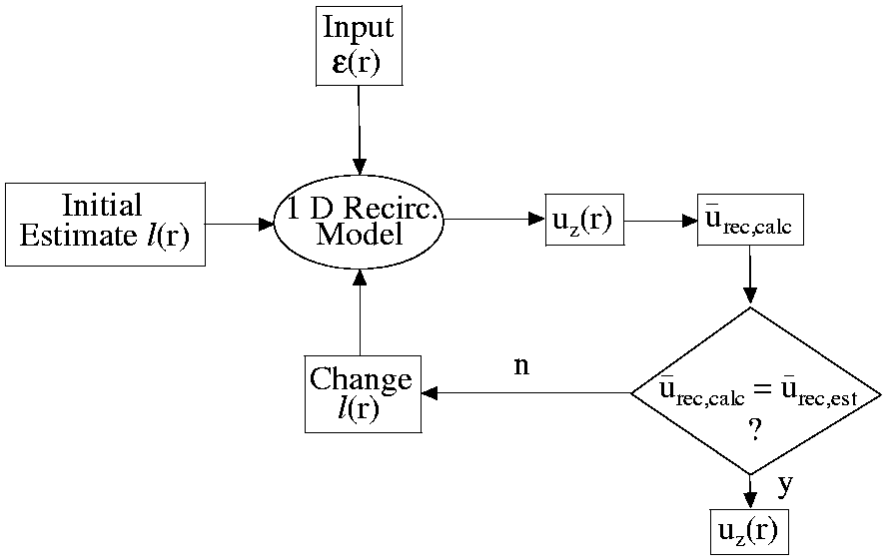

Figure 2.10 Determination of the Liquid Recirculating Velocity Profile, $u_z(r)$, with Knowledge of $\varepsilon_z(\xi)$ and $\bar{u}_{rec}$

The liquid (slurry) recirculation velocity profile evaluated in this manner is shown in Figure 2.11 for Run 14.6.

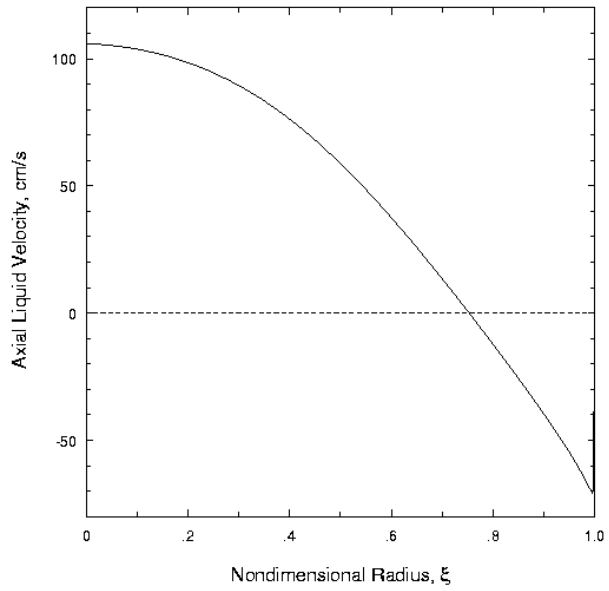

Figure 2.11 Calculated Axial Liquid Velocity Profile for Run 14.6, in the AFDU Reactor During Methanol Synthesis

The centerline velocity calculated is on the order of 1 m/s. Due to the large area and higher liquid holdup near the wall, the magnitude of the maximum downward liquid velocity is much

lower than the centerline velocity, in order to satisfy mass balance for the liquid (in batch mode). The radial profiles for the axial and radial eddy diffusivity are calculated from Equations 2.28 and 2.29, respectively, along with the estimated average values (Table 2.3).

$$D_{zz}(\xi) = \overline{D}_{ss} P_4$$

where $P_4 = -3.4979\xi^4 + 3.2704\xi^3 + 0.4693\xi^2 + 0.005035\xi + 0.5847$ (2.28)

$$D_{rr}(\xi) = \overline{D}_{rr} P_2$$

where $P_2 = -5.0929\xi^2 + 5.0717\xi + 0.1653$ (2.29)

The profiles for the axial and radial eddy diffusivities, calculated in this manner for Run 14.6, are shown in Figures 2.12 and 2.13, respectively.

Heat exchanger tubes are present in the AFDU reactor for cooling the medium. There are 24 one-inch (O.D.) tubes, which occupy approximately 7.5% of the cross-sectional area of the reactor, and extend over the entire length of the dispersion. The effect of the heat exchanger tubes is accounted for only with regard to the radial turbulent eddy diffusivity, since the presence of these tubes will physically reduce the radial length scales of turbulence. Liquid recirculation and the axial eddy diffusivity are assumed to be affected to a lesser extent, and for the current calculations, these effects are ignored.

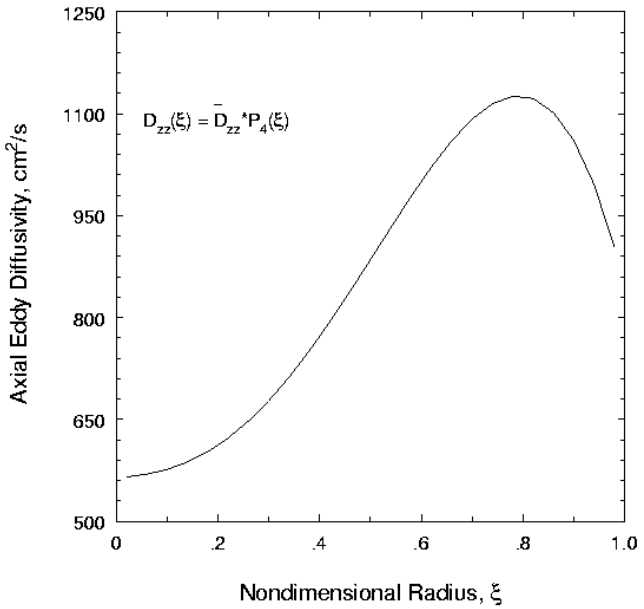

Figure 2.12 Calculated Axial Eddy Diffusivity Profile for Run 14.6, in the AFDU Reactor During Methanol Synthesis

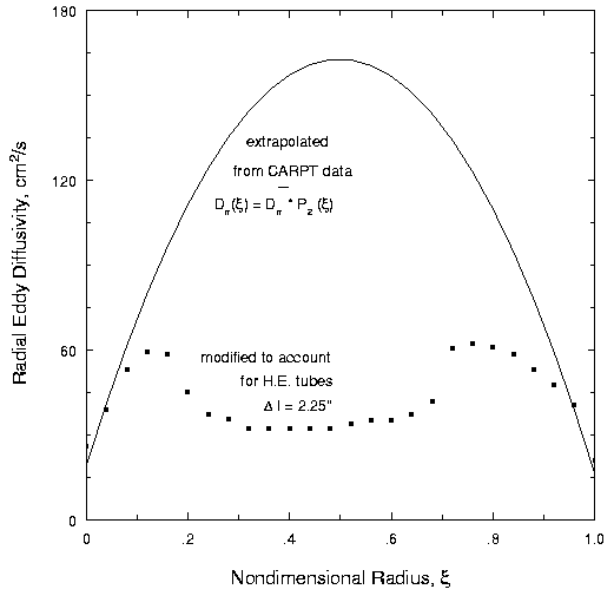

Figure 2.13 Calculated Axial Eddy Diffusivity Profile for Run 14.6, in the AFDU Reactor During Methanol Synthesis

A cross-sectional view of the reactor in the presence of these tubes is shown in Figure 2.14. The tubes are present in two annular rings about the center axis of the reactor, near the region of flow inversion, and will affect the radial turbulent diffusivities in this region by restricting the radial length scale of turbulence. This is accounted for by considering the characteristic spacing between the tubes, which is about 2.25 in. (5.7 cm), as an effective diameter and estimating the average radial diffusivity for this diameter (5.7 cm).

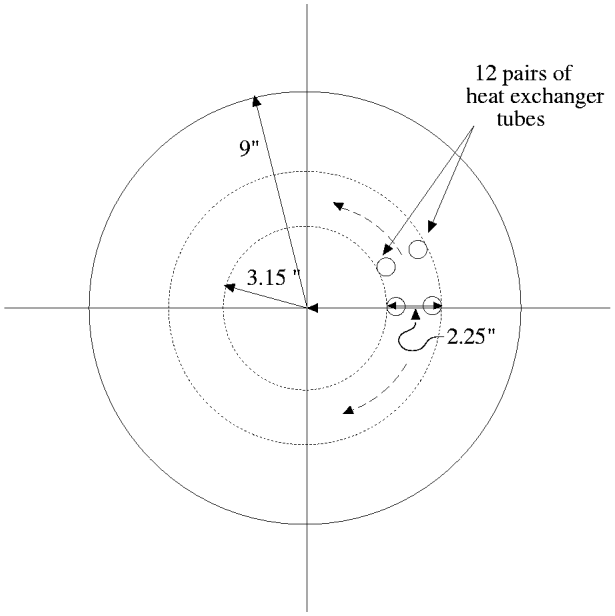

Figure 2.14 Schematic of the Cross-Sectional View of the AFDU Reactor showing Placement of Heat Exchanger Tubes

Equation 2.27, which was originally developed for large-diameter columns (>10 cm), is modified by retaining the 0.3 power dependence of D_{rr} on D_c and U_g (Equation 2.27) for smaller column diameters. With the CARPT data for the 14 cm diameter column as a reference, the following equation for the radial diffusivity for D_{ceff} = 5.7 cm is used:

$$\overline{D}_{rr(Dc=5.7)} = \left(\frac{5.7}{14.0}\right)^{0.3} \overline{D}_{rr(Dc=14)} \tag{2.30}$$

The above equation results in a radial diffusivity of 35 cm^2/s. The estimated value of the radial diffusivity in the region of the tubes, results in a modified profile for the radial eddy diffusivity, denoted by the dashed line in Figure 2.13. This represents a first approximation in accounting for the effect of heat exchanger tubes in the AFDU reactor. Thereby, all the input fluid dynamic parameters to the model are evaluated.

2.4.5 Simulation Results

The initial and boundary conditions are given below. Since the liquid is in batch mode, zero flux conditions are applied at all the boundaries.

$$r = 0,\ r = R; \quad \frac{\partial C}{\partial r} = 0 \tag{2.31}$$

$$z = 0,\ z = L; \quad \frac{\partial C}{\partial z} = 0 \tag{2.32}$$

The initial condition is assigned according to the location of tracer injection during an experiment. In the actual tracer experiment, the injection is made locally at a certain (r_i, θ_i, z_i). However, since the model is two dimensional, for modeling purposes the injection is considered to be made in an annular ring (r_i, z_i). The initial condition is given as:

$$\begin{aligned} t = 0; \quad C(r,z,t) &= f_t(t) \qquad r = r_i,\ z = z_i \\ &= 0 \qquad\quad r \neq r_i,\ z \neq z_i \end{aligned} \tag{2.33}$$

$f_t(t)$ describes the pulse of tracer injected (close to an impulse function), and is fitted to the response of the detector close to the location of injection. For a given experimental condition, four tracer experiments were carried out with four different locations of the injection point. These are provided in Table 2.2 (r_i and z_i are given in cm).

Table 2.2 Positions of Tracer Injection in the Model

	r_i (cm)	z_i (cm)
Wall injection at N1	22.8	966.0
Center injection at N1	11.5	966.0
Wall injection at N2	22.8	356.0
Center injection at N2	11.5	356.0

In order to compare the experimental results with model predictions, the individual detector responses measured by the four detectors at each axial level are averaged to yield an averaged detector response at each detector level. Averaging is done since the current model is only two dimensional, and cannot distinguish any angular variations in tracer concentration. Responses of the individual detectors at two axial levels indicate that such an (angular) averaging of the four detector responses at a given axial location is a reasonable approximation. The averaged experimental detector responses measured at the seven detector levels, for the wall injection at level N1 in Run 14.6, are shown in Figure 2.15. It is to be noted that the various detector level responses do not all show equal measurements at the end of long periods, which is what is expected if the tracer is eventually uniformly distributed in the reactor. Improper normalization of the detector responses caused this lack of uniformity. Specific details and reasons for this are shown elsewhere (Degaleesan, 1997), where suggestions have been made to improve the quality of the tracer data. Due to this lack of uniformity, the experimental detector responses cannot be quantitatively compared with the model predictions of the tracer distribution in the column. Only the characteristic mixing times as measured by the times of the peaks of the curves can be compared.

The radiation intensity emitted per unit volume by the tracer is directly proportional to the tracer concentration. Since the experiments involve radioactive tracer, the measurements, as detected by the scintillation detectors, represent neither local nor average tracer concentration, but the attenuated cumulative tracer concentration in a given cross-sectional plane.

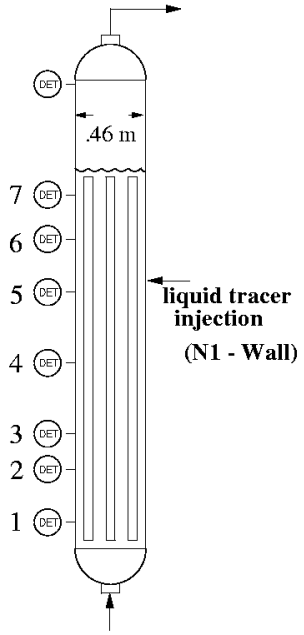

Figure 2.15 (a) Position of Liquid Tracer Injection to Wall of Reactor for Tracer Experiments

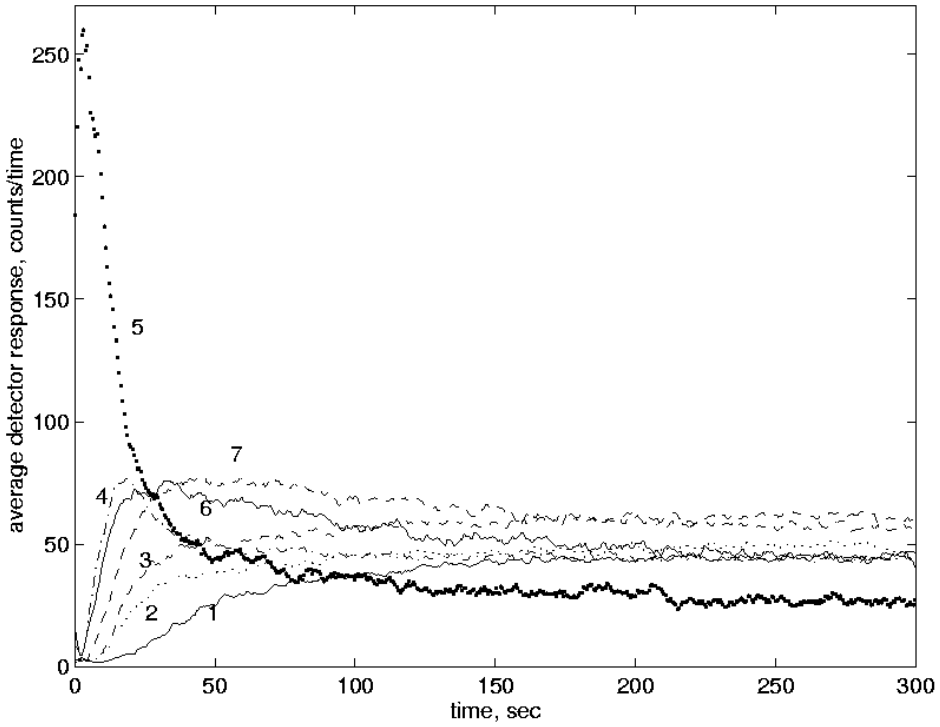

Figure 2.15 (b) Experimental Detector Responses for Wall Injection at Level N1 for Run 14.6

The detectors are shielded on their sides. Hence, most of the radiation detected emanates from the cross-sectional plane at the axial level of the detector. In order to compare the model predictions with the averaged experimental detector response, the local tracer concentration in a two-dimensional axisymmetric domain, *C(r,z,t),* is first integrated along the radial path *r* through the column center, using the Beer-Lambert law, to yield a representative radioactive tracer response at a given axial location, $\breve{C}(z,t)$. Therefore,

$$\breve{C}(z,t) = \int_{r'=0}^{r'=R} C(r',z,t) \exp\left(-\int_{r'}^{R} \mu_{eff}(r'')dr'' \right) dr' \tag{2.34}$$

where

$$\mu_{eff}(r) = \mu_g \varepsilon_g(r) + \mu_{sl} \varepsilon_{sl}(r) \tag{2.35}$$

$\breve{C}(z,t)$ represents the response measured by the shielded and collimated detectors, which have been used for the current experiments. Since the detectors are collimated, the only significant contribution of the radiation that is measured emanates from the tracer along the radial path *r* through the column center. Hence, the contribution from the angular and axial direction is ignored in the calculations. The Mn^{56} particles emit γ radiation at 0.85 MeV. The catalyst loading in the reactor for all three runs was kept at a constant of 40% by weight. For a given

composition of the catalyst particles resulting in a bulk density ρ_s = 2.02 gm/cm^3, and liquid (hydrocarbon oil) density of ρ_l = 0.667 gm/cm^3, the linear attenuation coefficient of the slurry at 0.85 MeV is μ_{sl} = 0.06728 cm^{-1}, and for the gas it is μ_g = 1.0e-5 cm^{-1}.

Figures 2.16 and 2.17 compare model predictions with the experimental tracer responses for the wall injection at level N1 for Run 14.6. The calculated as well as the measured responses have been normalized with respect to their maximum for the sake of comparison. The results show that the model is able to capture the characteristic overshoots as seen by the detector responses at all the measurement levels. A quantitative comparison of the tracer responses is unfortunately not possible due to the fact that the experimental data do not level off at the end of long periods at the same height for all the detectors.

Figures 2.18 and 2.19 compare model predictions and experimental detector responses for the center injection at level N2, and Figure 2.20 compares them at level N1 (Figure 2.9). Experimental data at Levels 5, 6 and 7 for center injection at N1 and at all levels for the wall injection at N2 in Run 14.6 were not available for comparison. For all the different locations of injection, since the operating process conditions are the same, the input model parameters are fixed. Therefore, with a consistent set of model parameters, the model is able to capture the internal liquid (slurry) and overall mixing in the AFDU reactor, as measured by the detector responses at all seven locations. Table 2.3 lists the average input parameters calculated for all three experimental conditions considered. The radial profiles for liquid velocity and turbulent diffusivities were obtained using the developed scaleup procedure.